Ultrafast Infrared Heating Laser Pulse-Induced Micellization Kinetics of Poly(ethylene oxide)−Poly(propylene oxide)−Poly(ethylene oxide) in Water

Xiaodong Ye,[†] Yijie Lu,[†] Shilin Liu,*[,†] Guangzhao Zhang,[†] and Chi Wu*[,†,‡]

The Hefei National Laboratory for Physical Sciences at Microscale and Department of Chemical Physics, University of Science and Technology of China, Hefei, Anhui 230026, China, and Department of Chemistry, The Chinese University of Hong Kong, Shatin N.T., Hong Kong

Received June 4, 2007. In Final Form: July 7, 2007

The heating-induced micellization of poly(ethylene oxide)-*b*-poly(propylene oxide)-*b*-poly(ethylene oxide) (Pluronic PE10300) triblock copolymer chains was studied by ultrasensitive differential scanning calorimetry, laser light scattering, and fluorescence spectrometry with a fluorescent probe, 8-anilino-1-naphthalenesulfonic acid ammonium salt. The critical micellization temperatures obtained from the three methods are similar. The micellization kinetics was studied in terms of changes in the fluorescence and Rayleigh scattering intensities after an ultrafast infrared heating laser pulse (∼10 ns)-induced temperature jump. The increases in the fluorescence and Rayleigh scattering intensities in the millisecond range can be well described by a single-exponential equation, corresponding to the incorporation of individual triblock copolymer chains (unimers) into large spherical micelles. The increase in copolymer concentration or the initial solution temperature decreases the characteristic transition time. In general, the fluorescence measurement has a better signal-to-noise ratio but leads to a transition time that is slightly shorter than that from the corresponding Rayleigh scattering measurement for a given copolymer solution.

Introduction

Triblock copolymer poly(ethylene oxide)-*b*-poly(propylene oxide)-*b*-poly(ethylene oxide) (PEO−PPO−PEO) has received much attention because of its industrial applications in detergents, stabilizers, emulsifiers, and formulation agents in cosmetics. Furthermore, as a potential biomedical material, its amphiphilic nature and low toxicity are also attractive.[1,2] The PPO/PEO ratio and chain length can be varied to meet the specific requirements of different applications. In dilute aqueous solutions, it often forms a spherical micelle-like microstructure with a hydrophobic collapsed PPO core and a hydrophilic swollen PEO shell at higher temperatures. For each given copolymer composition, there normally exists a critical micellization concentration (C_{CMC}) for a given temperature and a critical micellization temperature (T_{CMT}) for a given copolymer concentration. In the last two decades, micellization under different conditions has been extensively studied with different methods, including differential scanning calorimetry,[3−9] laser light scattering,[10−14] fluorescence and Raman spectroscopy,[15−20] neutron scattering,[21−24] and surface tension.[25−27] The properties of these copolymers at equilibrium are well understood.[28−30]

On the other hand, some kinetic studies of micellization by various methods have also been reported. These methods include Joule heating,[31−34] temperature jump,[35−38] stopped flow,[37,39] and

* Corresponding author. E-mail: chiwu@cuhk.edu.hk.
† University of Science and Technology of China.
‡ The Chinese University of Hong Kong.

(1) Kabanov, A. V.; Alakhov, V. Y. *Crit. Rev. Ther. Drug* **2002**, *19*, 1.
(2) Kabanov, A. V.; Batrakoval, E. V.; Sherman, S.; Alakhov, V. Y. *Adv. Polym. Sci.* **2006**, *193*, 173.
(3) Wanka, G.; Hoffmann, H.; Ulbricht, W. *Colloid Polym. Sci.* **1990**, *268*, 101.
(4) Mitchard, N.; Beezer, A.; Rees, N.; Mitchell, J.; Leharne, S.; Chowdhry, B.; Buckton, G. *J. Chem. Soc., Chem. Commun.* **1990**, *13*, 900.
(5) Armstrong, J. K.; Parsonage, J.; Chowdhry, B.; Leharne, S.; Mitchell, J.; Beezer, A.; Löhner, K.; Laggner, P. *J. Phys. Chem.* **1993**, *97*, 3904.
(6) Alexandridis, P.; Nivaggioli, T.; Hatton, T. A. *Langmuir* **1995**, *11*, 1468.
(7) Alexandridis, P.; Holzwarth, J. F. *Langmuir* **1997**, *13*, 6074.
(8) Couderc, S.; Li, Y.; Bloor, D. M.; Holzwarth, J. F.; Wyn-Jones, E. *Langmuir* **2001**, *17*, 4818.
(9) Batsberg, W.; Ndoni, S.; Trandum, C.; Hvidt, S. *Macromolecules* **2004**, *37*, 2965.
(10) Zhou, Z. K.; Chu, B. *Macromolecules* **1987**, *20*, 3089.
(11) Reddy, N. K.; Fordham, P. J.; Attwood, D.; Booth, C. *J. Chem. Soc., Faraday Trans.* **1990**, *86*, 1569.
(12) Zhou, Z. K.; Chu, B. *J. Colloid Interface Sci.* **1988**, *126*, 171.
(13) Brown, W.; Schillén, K.; Almgren, M.; Hvidt, S.; Bahadur, P. *J. Phys. Chem.* **1991**, *95*, 1850.
(14) Chu, B. *Langmuir* **1995**, *11*, 414.
(15) Kabanov, A. V.; Nazarova, I. R.; Astafieva, I. V.; Batrakova, E. V.; Alakhov, V. Y.; Yaroslavov, A. A.; Kabanov, V. A. *Macromolecules* **1995**, *28*, 2303.
(16) Vasilescu, M.; Caragheorgheopol, A.; Caldararu, H.; Bandula, R.; Lemmetyinen, H.; Joela, H. *J. Phys. Chem. B* **1998**, *102*, 7740.
(17) Nakashima, K.; Takeuchi, K. *Appl. Spectrosc.* **2001**, *55*, 1237.
(18) Guo, C.; Wang, J.; Liu, H. Z.; Chen, J. Y. *Langmuir* **1999**, *15*, 2703.
(19) Guo, C.; Liu, H. Z.; Wang, J.; Chen, J. Y. *J. Colloid Interface Sci.* **1999**, *209*, 368.
(20) Almgren, M.; Alsins, J.; Bahadur, P. *Langmuir* **1991**, *7*, 446.
(21) Wu, G. W.; Chu, B.; Schneider, D. K. *J. Phys. Chem.* **1995**, *99*, 5094.
(22) Goldmints, I.; von Gottberg, F. K.; Smith, K. A.; Hatton, T. A. *Langmuir* **1997**, *13*, 3659.
(23) Mortensen, K. *J. Phys.: Condens. Matter* **1996**, *8*, A103.
(24) Mortensen, K.; Pedersen, J. S. *Macromolecules* **1993**, *26*, 805.
(25) Alexandridis, P.; Hatton, T. A. *Colloids Surf., A* **1995**, *96*, 1.
(26) Alexandridis, P.; Athanassiou, V.; Fukuda, S.; Hatton, T. A. *Langmuir* **1994**, *10*, 2604.
(27) Alexandridis, P.; Nivaggioli, T.; Hatton, T. A. *Langmuir* **1995**, *11*, 1468.
(28) Almgren, M.; Brown, W.; Hvidt, S. *Colloid Polym. Sci.* **1995**, *273*, 2.
(29) Almgren, M.; Bahadur, P.; Jansson, M.; Li, P. Y.; Brown, W.; Bahadur, A. *J. Colloid Interface Sci.* **1992**, *151*, 157.
(30) Chu, B.; Zhou, Z. K. Physical Chemistry of Polyoxyalkylene Block Copolymer Surfactants. In *Nonionic Surfactants: Polyoxyalkylene Block Copolymer Studies*; Nace, V. M., Ed.; Marcel-Dekker: New York, 1996; Chapter 3, pp 67−143.
(31) Hecht, E.; Hoffmann, H. *Colloids Surf., A* **1995**, *96*, 181.
(32) Michels, B.; Waton, G.; Zana, R. *Langmuir* **1997**, *13*, 3111.
(33) Waton, G.; Michels, B.; Zana, R. *J. Colloid Interface Sci.* **1999**, *212*, 593.
(34) Waton, G.; Michels, B.; Zana, R. *Macromolecules* **2001**, *34*, 907.
(35) Goldmints, I.; Holzwarth, J. F.; Smith, K. A.; Hatton, T. A. *Langmuir* **1997**, *13*, 6130.
(36) Kositza, M. J.; Bohne, C.; Alexandridis, P.; Hatton, T. A.; Holzwarth, J. F. *Langmuir* **1999**, *15*, 322.
(37) Kositza, M. J.; Bohne, C.; Alexandridis, P.; Hatton, T. A.; Holzwarth, J. F. *Macromolecules* **1999**, *32*, 5539.
(38) Kositza, M. J.; Rees, G. D.; Holzwarth, A.; Holzwarth, J. F. *Langmuir* **2000**, *16*, 9035.

10.1021/la701626k CCC: $37.00
Published on Web 08/18/2007

the ultrasonic relaxation.[32,33,40] The results reveal more than one kinetic processes.[32−37] The fast one is in the range of 0.02−1 ms, which was attributed to the incorporation of individual triblock copolymer chains (unimers) into large spherical micelles. Holzwarth and co-workers[36,37] suggested that another process in the range of 0.2−100 ms might be related to micelle restructuring and the slowest one occurring near the cloud point could be attributed to intermicelle aggregation or fusion. However, Zana and co-workers[32,34] thought that both the second and third processes could be due to the formation and breakage of large micelles.

Note that the previously used fluorescent probe, 1,6-diphenyl-1,3,5-hextriene (DPH), is hydrophobic and mainly located inside the insoluble hydrophobic PPO core, reflecting the microenvironmental change bearing the PPO block. This is why Holzwarth and co-workers found that the fluorescence intensity remained a constant before increasing to a maximum in the second stage. In this study, we choose the hydrophilic 8-anilino-1-naphthalenesulfonic acid ammonium salt (ANS) as a fluorescent probe to study the formation kinetics of the hydrophilic PEO shell during micellization by using our homebuilt fluorescence spectrometer equipped with an ultrafast pulsed infrared heating laser (∼10 ns). We can measure both the fluorescence and Rayleigh scattering intensities. The characteristic transition times determined from the changes in both intensities are compared.

Experimental Section

Materials. Poly(ethylene oxide)-*b*-poly(propylene oxide)-*b*-poly(ethylene oxide) triblock copolymer (PE10300) was kindly provided by BASF AG, Ludwigshafen, Germany. The listed weight content of PEO (W_{PEO}) is 30%, and the molar mass of PPO (M_{PPO}) is 3250 g/mol. The copolymer was purified by six extractions with hexane to remove impurities, including diblock PEO−PPO chains. The copolymer purity was checked by dynamic laser light scattering until no extra peak was observed in the measured characteristic relaxation time distribution at higher temperatures. *Note that such a purification process is vitally important for a credible study of this kind of triblock copolymer.* After purification, H-NMR shows a slightly different characterization in comparison with that of the unpurified copolymer, namely, $W_{PEO} = 33$ wt %, $M_{PE10300}$(LLS) = 6.0×10^3 g/mol, $M_{PE10300}$(GPC) = 6.5×10^3 g/mol, and M_w/M_n (GPC) = 1.17. From M_w (LLS) and M_w/M_n (GPC), we estimated the average structure of purified PE10300 to be $EO_{19}PO_{60}EO_{19}$. Water distilled three times was used as the solvent. A stock solution of ANS (10.6 mM) was prepared by directly dissolving ANS in water. Each solution mixture of PE10300 and ANS was prepared by adding the ANS stock solutions to an aqueous solution of PE10300 under stirring. The final ANS concentration was determined by using the adsorption at 350 nm with an extinction coefficient of 5×10^3 M^{-1} cm^{-1}.[41,42]

Laser Light Scattering. A commercial LLS spectrometer (ALV/DLS/SLS-5022F) equipped with a multi-τ digital time correlator (ALV5000) and a cylindrical 22 mW UNIPHASE He−Ne laser (λ_0 = 632.8 nm) as the light source was used. In static LLS,[43,44] the angular dependence of the absolute excess time-average scattering intensity, known as the Rayleigh ratio $R_{vv}(q)$, was recorded, and we were able to obtain the weight-average molar mass (M_w), the root-mean-square radius of gyration $\langle R_g^2\rangle_z^{1/2}$ (or $\langle R_g\rangle$), and the second virial coefficient (A_2) by using

$$\frac{K(C - C_{CMC})}{R_{vv}(q)} = \frac{1}{M_w}\left(1 + \frac{1}{3}\langle R_g^2\rangle_z q^2\right) + 2A_2(C - C_{CMC}) \quad (1)$$

where $K = 4\pi^2(dn/dC)^2/(N_A\lambda_0^4)$ and $q = (4\pi n/\lambda_0)\sin(\theta/2)$ with C, dn/dC, N_A, and λ_0 being concentration of the polymer, the specific refractive index increment, Avogadro's number, and the wavelength of light in vacuum, respectively. The refractive index increment (dn/dC = 0.124 mL g^{-1}) of PE10300 in water was measured by using a novel differential refractometer at 28 °C and 633 nm.[45] C_{CMC} is the critical micellization concentration of the copolymer at a certain temperature. In this study, $\langle R_g^2\rangle q^2$ is much smaller than 1. In dynamic LLS, the Laplace inversion of a measured intensity−intensity time correlation function [$G^{(2)}(t, q)$] in the self-beating mode can result in a line-width distribution of [$G(\Gamma)$]. For a pure diffusive transition, Γ is related to the translational diffusion coefficient D by $\Gamma/q^2 = D$ at $q \to 0$ and $C \to 0$ or a hydrodynamic radius R_h by $R_h = k_BT/(6\pi\eta D)$ with k_B, T, and η being the Boltzman constant, absolute temperature, and solvent viscosity, respectively.

Fast Infrared Laser Heating. The second harmonic (532 nm) of an Nd:YAG laser (Spectra Physics, Lab-170, 10 Hz) is filtered with ∼71% pass of its fundamental emission at 1.064 μm. An optical isolator including a thin-film polarizer and a quarter wave plate is placed behind the filter to prevent the leakage of backward 1.064 μm radiation and Brillouin scattering into the laser.[46] The laser beam is then focused into one Raman cell made of a stainless steel tube with two quartz windows (80 cm in length, 26 mm in diameter, filled with 40 atm of methane). The emerging beam, consisting of a seed 1.54 μm laser pulse and some remaining fundamental emission at 1.064 μm, is collimated and refocused by two lenses (f = 500 mm) into another Raman cell (100 cm in length, 26 mm in diameter, filled with 40 atm of methane).[47−49] Residual pumping light is removed by a dichroic mirror mounted at ∼45° reflecting most of the 1.54 μm light while allowing more than 92% of the 1.064 μm light to pass. Finally, two such dichroic mirrors are used to direct the pulsed 1.54 μm laser beam into the solution, providing a further reduction of the Nd:YAG fundamental emission. In this way, conversion to higher-order Stokes and anti-Stokes lines as well as the intensity fluctuation of 1.54-μm light, are suppressed efficiently. A filter is also used to pass ∼90% of the 1.54 μm light but absorb most of visible light so that the effect of anti-Stokes lines is minimized.[49] Such converted laser heating pulses (1.54 μm, ∼2 mJ/pulse at 10 Hz) can induce a fast temperature jump of an aqueous solution as a result of its absorption by the overtone of the O−H stretching vibration in H_2O.[50−52] The laser pulse is focused into the middle of the solution with a cross section of ∼0.8 mm^2 by a lens (f = 800 mm). Note that the fluorescence and light-scattering volumes are much smaller and are located in the center of the heated volume.

A 200-W high-pressure mercury lamp (Shanghai Hualun Bulk Factory) as the fluorescence and light-scattering light source is used. We used a heat filter (GRB3, from Jiangsu Haian Yaguang Scientific & Educational Equipment, China) to absorb the infrared radiation. Two quartz lenses (f = 50 and 90 mm) are used to collect and collimate the photon flux from the light source. A filter with a transmitting window (245−400 nm) is placed behind the second lens (f = 50 mm). One pinhole (1 mm) is used to reduce the size of the incident facula. A lens (f = 30 mm) located in the middle of the pinhole and the center of the solution in a $2f-2f$ configuration is used to transfer the probe beam into the solution. The fluorescence or the scattered light is collected by two quartz lenses (f = 40 and

(39) Kositza, M. J.; Bohne, C.; Hatton, T. A.; Holzwarth, J. F. *Prog Colloid Polym. Sci.* **1999**, *112*, 146.
(40) Thurn, T.; Couderc-Azouani, S.; Bloor, D. M.; Holzwarth, J. F.; Wyn-Jones, E. *Langmuir* **2003**, *19*, 4363.
(41) Shastry, M. C. R.; Udgaonkar, J. B. *J. Mol. Biol.* **1995**, *247*, 1013.
(42) Kumar, Y.; Muzammilt, S.; Tayyab, S. *J. Biochem.* **2005**, *138*, 335.
(43) Zimm, B. H. *J. Chem. Phys.* **1948**, *16*, 1099.
(44) Chu, B. *Laser Light Scattering*, 2nd ed., Academic Press: New York, 1991.
(45) Wu, C.; Xia, K. Q. *Rev. Sci. Instrum.* **1994**, *65*, 587.
(46) Kazzaz, A.; Ruschin, S.; Shoshan, I.; Ravnitsky, G. *IEEE J. Quantum Electron.* **1994**, *30*, 3017.
(47) Ameen, S. *Rev. Sci. Instrum.* **1975**, *46*, 1209.
(48) Wang, J. P.; Gan, D. J.; Lyon, L. A.; El-Sayed, M. A. *J. Am. Chem. Soc.* **2001**, *123*, 11284.
(49) Yamamoto, K.; Mizutani, Y.; Kitagawa, T. *Biophys. J.* **2000**, *79*, 485.
(50) Turner, D. H.; Flynn, G. W.; Sutin, N.; Beitz, J. V. *J. Am. Chem. Soc.* **1972**, *94*, 1554.
(51) Turner, D. H.; Flynn, G. W.; Lundberg, S. K.; Faller, L. D.; Sutin, N. *Nature* **1972**, *239*, 215.
(52) Williams, A. P.; Longfellow, C. E.; Freier, S. M.; Kierzek, R.; Turner, D. H. *Biochemistry* **1989**, *28*, 4283.

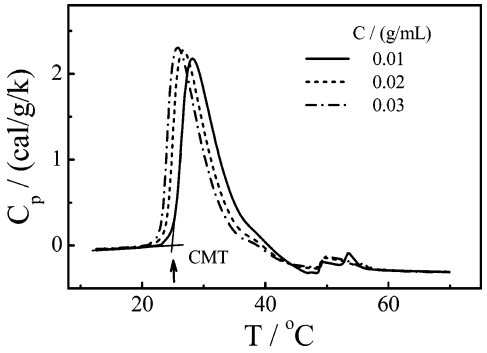

Figure 1. Temperature dependence of the specific heat capacity (C_p) of different PE10300 aqueous solutions, where the arrow shows how critical micellization temperature (CMT) is determined.

50 mm). Another pinhole (1 mm) is placed in front of a photomultiplier tube (PMT, R928, Hamamatsu) to eliminate some stray light. A cutoff filter (450 nm) and a heat filter (GRB3) are placed in front of the PMT. The sample cell consisting of a pair of quartz windows with a 200-μm spacer is thermally controlled to a precision of $\pm$0.1 °C by a heating bath.

Each heating laser pulse jumps the solution temperature and shifts the unimer $\leftrightarrow$ micelle equilibrium. The transition kinetics can be studied by monitoring the change in fluorescence (ANS) intensity or Rayleigh scattering intensity. Each data point was normally averaged over measurements repeated 512 times so that the signal-to-noise ratio was improved. Using a 5.6-kΩ matched resistance, we are able to observe the change in fluorescence or Rayleigh light scattering intensity of aqueous solutions with a short dead time of $\sim$2 μs.

Differential Scanning Calorimetry and Fluorescence Spectrometry. An ultrasensitive DSC (VP DSC from MicroCal) was used. The volume of the sample cell was 0.509 mL. The reference cell was filled with deionized water. PE10300 solutions were degassed at 25 °C for half an hour. The heating rate was 1.00 °C/min. The fluorescence spectra were recorded on an LS-55 spectrophotometer by using a quartz cell with an optical path length of 0.5 mm. The temperature of the samples was monitored by a thermometer with a precision of $\pm$0.1 °C.

Results and Discussion

We first studied the micellization of PEO−PPO−PEO in aqueous solution by using ultrasensitive differential scanning calorimetry (US-DSC), a sensitive method for measuring the energy change in polymer association.[53,54] Figure 1 shows the temperature dependence of the specific heat capacity (C_p) of different PE10300 aqueous solutions. The endothermic peak indicates the dehydration of PPO at higher temperatures during micellization. The arrow in Figure 1 shows how the critical micellization temperature (T_{CMT}) is defined in our DSC experiments. It is clear that T_{CMT} decreases as the copolymer concentration increases.

Figure 2 summarizes how T_{CMT} depends on the PE10300 concentration. The line represents the $C_{CMC}-T_{CMT}$ boundary, dividing two different phases, namely, individual copolymer chains (unimers) without any micelle and the coexistence of micelles and unimers, where C_{CMC} is the critical micellization concentration for a given temperature. Quantitatively, $T_{CMT} = (17.3 \pm 0.2) - (3.8 \pm 0.1)lg(C_{CMC})$ in the temperature range of 23.0−31.0 °C. Besides DSC, we also studied micellization by using laser light scattering (LLS) and static fluorescence spectroscopy.

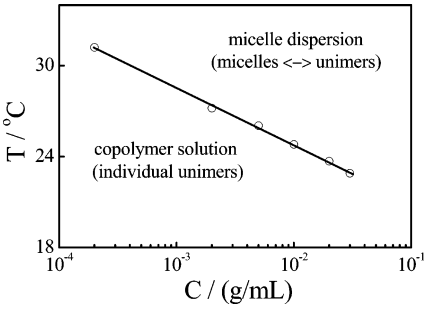

Figure 2. Phase diagram of PE10300 aqueous solutions, where the line shows the boundary between the copolymer solution and the micelle dispersion.

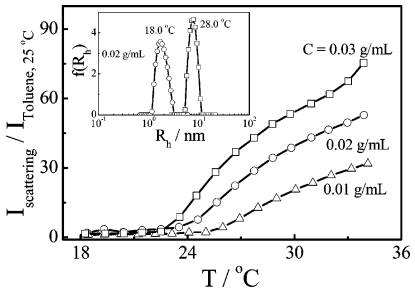

Figure 3. Temperature dependence of the relative scattered light intensity of different PE10300 aqueous solutions. The inset shows intensity distributions of the hydrodynamic radius in one PE10300 aqueous solution at two different temperatures.

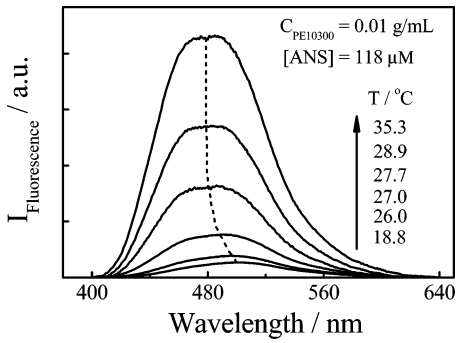

Figure 4. Temperature dependence of the fluorescence emission spectra of the hydrophilic fluorescent probe (ANS) in one PE10300 aqueous solution, where λ_{ex} = 365 nm.

Figure 3 shows the temperature dependence of the relative Rayleigh scattering intensity ($I/I_{toluene}$) of different PE10300 aqueous solutions. At lower temperatures, $I/I_{toluene}$ is nearly a constant, indicating the existence of only individual chains with an average hydrodynamic radius ($\langle R_{h,0}\rangle$) of $\sim$1.8 nm at infinite dilution. The increase in $I/I_{toluene}$ in the higher temperature range reflects interchain association (i.e., micellization). Note that $\langle R_h\rangle$ also abruptly increases and approaches $\sim$7 nm at higher temperatures, as shown in the inset, and the average hydrodynamic radius ($\langle R_{h,0}\rangle$) becomes $\sim$7.5 nm at infinite dilution. Both the unimers and the resultant micelles are narrowly distributed, similar to literature values.[55]

Figure 4 shows the temperature dependence of fluorescence emission spectra of ANS in aqueous solutions of PE10300. Note that ANS shows no fluorescence in pure water but is highly fluorescent in a low polar environment. The dotted line shows the blue shift of the maximum in the emission spectra with increasing temperature because micellization traps a small amount of ANS in the hydrophobic PPO core even though most of them

(53) Schild, H. G.; Tirrell, D. A. *J. Phys. Chem.* **1990**, *94*, 4352.
(54) Ding, Y. W.; Ye, X. D.; Zhang, G. Z. *Macromolecules* **2005**, *38*, 904.
(55) Zhou, Z. K.; Chu, B. *Macromolecules* **1988**, *21*, 2548.

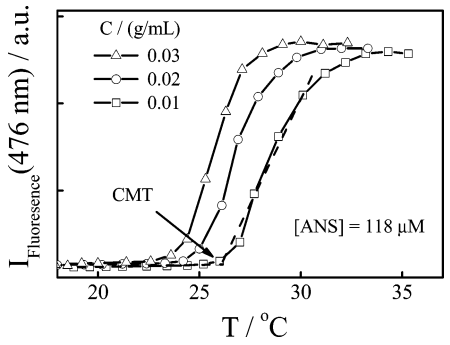

Figure 5. Temperature dependence of the fluorescence intensity ($\lambda_{emission} = 476$ nm) of hydrophilic fluorescent probe (ANS) in one PE10300 aqueous solution.

Table 1. Critical Micellization Temperatures (T_{CMT}) Determined by Differential Scanning Calorimetry, Laser Light Scattering, and Static Fluorescence Measurement.

$C_{PE10300}$	0.01 g/mL	0.02 g/mL	0.03 g/mL
T_{CMT} (DSC)	24.8	23.7	22.9
T_{CMT} (LLS)	25.0	23.7	22.7
T_{CMT} (fluorescence)[a]	26.0	24.9	23.7

[a] The concentration of the hydrophilic fluorescent probe (ANS) is fixed at 118 μM.

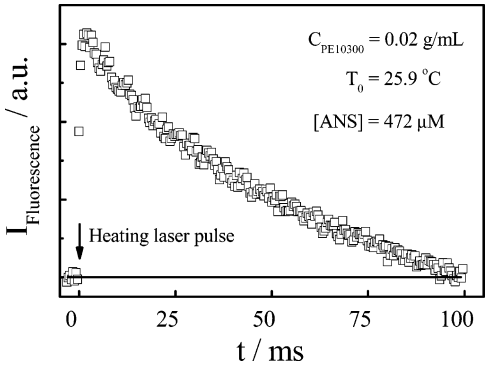

Figure 6. Temperature jump-induced change in fluorescence intensity of a hydrophilic fluorescent probe (ANS) in one PE10300 aqueous solution.

are inside the hydrophilic PEO shell. The trapping as well as the dehydration of the hydrophilic PEO shell decreases the polarity around ANS. It is this unique property that makes ANS a widely used probe for the polarity evaluation of its binding sites.[56]

Figure 5 shows that the fluorescence intensity at 476 nm remains nearly constant in the low-temperature range. T_{CMT}, marked by the sudden increase in fluorescence intensity, decreases as the copolymer concentration increases, similar to the results in Figure 3. As shown in Table 1, there is no significant difference among the values of T_{CMT} from different methods. It should be stated that the values of T_{CMT} listed in Table 1 are 3−5 °C higher than those reported for a similar triblock copolymer (P103, $M_{PPO} = 3465$ g/mol and $W_{PEO} = 30\%$).[57] The higher T_{CMT} may reflect a small difference in the copolymer composition and/or sample purification. After establishing the above relations between the copolymer concentration and T_{CMT}, we studied the micellization kinetics by measuring the time dependence of the fluorescence intensity after the fast laser heating pulse.

Figure 6 shows the typical time dependence of the fluorescence intensity after the heating laser pulse-induced temperature jump.

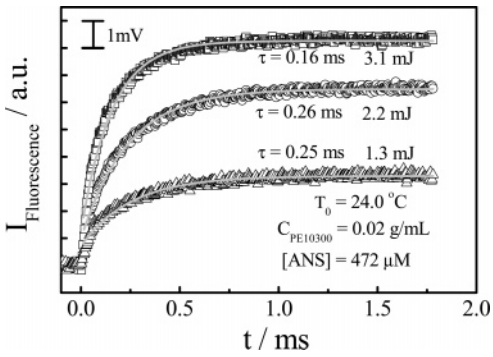

Figure 7. Time dependence of temperature jump-induced change in fluorescence intensity of a hydrophilic fluorescent probe (ANS) in one PE10300 aqueous solution under different laser powers.

The fluorescence intensity sharply increases within a few milliseconds, which is what we are interested in. The complete relaxation back to its original level after ~100 ms reflects the heat dissipation and the dissolution of large micelles back into individual copolymer chains and small micelles before the next heating laser pulse. Therefore, we set the time interval between two heating laser pulses to be 100 ms to ensure no residual heating effect when the second laser pulse comes. In this way, we are able to repeat our measurements many times and average them to increase the signal-to-noise ratio.

Figure 7 shows an enlargement of the initial time dependence of fluorescence intensity after the solution is irradiated with different laser powers. All of the curves are well fitted by a single-exponential function

$$\frac{I_F(t) - I_F(0)}{I_F(\infty) - I_F(0)} = 1 - e^{-t/\tau} \qquad (2)$$

where t, 0, and ∞ denote fluorescence intensities at time $t = t$, 0, and ∞, respectively; t is the time after the heating pulse, and τ is the characteristic transition time. The fitting of each set of experimental data points with eq 2 leads to a value of τ that is nearly constant when the laser power is lower than 2.2 mJ but decreases as the laser power further increases. This is reasonable because a higher heating power leads to a deeper quench into the phase-transition region so that the transition becomes faster. In this study, we made a compromise between the quenching depth and a sufficient signal-to-noise ratio, namely, keeping the laser power (I_0) at 2.2 mJ, which can lead to a temperature jump (ΔT) of ~1 °C, estimated on the basis of the absorption of electromagnetic radiation at 1.54 μm and $\Delta T = I_o[1 - \exp(-2.303AL)]/cL$, where I_0 is the incident radiation intensity (cal·cm^{-2}), c is the heat capacity of the medium in cal·cm^{-3}·deg^{-1}, L is the length of the heating path, and A is the medium's absorbance per cm. In this study, $c = 1$ cal·cm^{-3}·deg^{-1}, $L = 0.02$ cm, $I = 0.066$ cal·cm^{-2}, and $A = 5.3$ cm^{-1}.[58] Such a temperature jump can change the fluorescence intensity by up to 6%. Note that the association rate (k^+) is obtainable because the laser heating rate is much faster than the association rate. However, the heat-dissipating rate is slower than the micelle dissociation rate. This is why we cannot measure the dissociation rate (k^-) from the intensity decay in Figure 6.

Figure 8 summarizes the initial temperature dependence of the characteristic transition time in the presence of different amounts of ANS. It is clear that the ANS concentration has nearly no effect on the micellization kinetics of PE10300 in aqueous solutions. We can also monitor the micellization kinetics

(56) Azzi, A. *Methods Enzymol.* **1974**, *32*, 234.
(57) Alexandridis, P.; Holzwarth, J. F.; Hatton, T. A. *Macromolecules* **1994**, *27*, 2414.
(58) Palmer, K. F.; Williams, D. *J. Opt. Soc. Am.* **1974**, *64*, 1107.

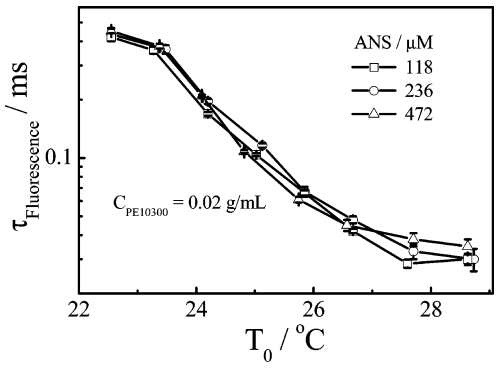

Figure 8. Initial solution temperature (T_0) dependence of the characteristic transition time (τ) of one PE10300 aqueous solution with different amounts of fluorescent probe ANS.

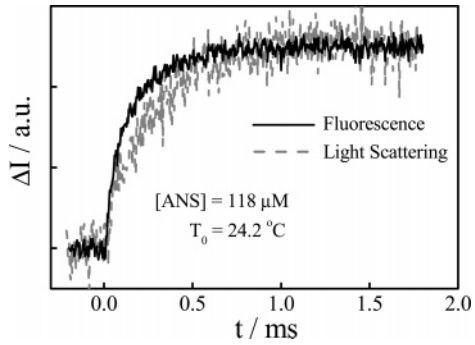

Figure 9. Time dependence of Rayleigh scattering and fluorescence intensities from one PE10300 aqueous solution after the heating laser pulse-induced temperature jump.

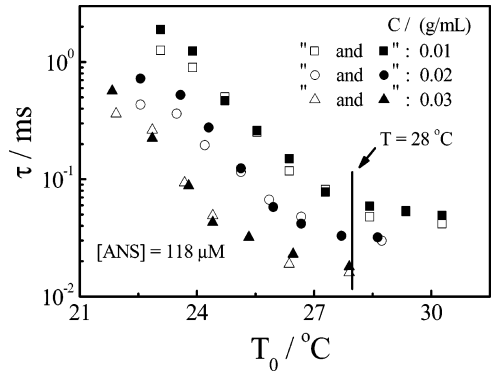

Figure 10. Initial solution temperature (T_0) dependence of characteristic transition times (τ), respectively, determined from temperature jump-induced changes in Rayleigh scattering (filled symbols) and fluorescence (open symbols) intensities of three PE10300 aqueous solutions.

by measuring the Rayleigh scattering intensity. Figure 9 shows a comparison of the results from the fluorescence and Rayleigh scattering intensities. The characteristic relaxation time determined from the Rayleigh scattering is longer than that from the fluorescence measurement. Note that the signal-to-noise ratio in the fluorescence measurement is higher than that in the Rayleigh scattering measurement. This is because in the Rayleigh scattering measurement a higher voltage was applied to the PMT to increase the output signal strength so that noise also increases.

Figure 10 shows that the characteristic transition time decreases as the initial temperature or the polymer concentration increases either in the Rayleigh scattering or in the fluorescence measurement. Note that the two methods result in similar values of τ for each given initial temperature. Therefore, in comparison with using a hydrophobic DPH fluorescent probe in previous studies,

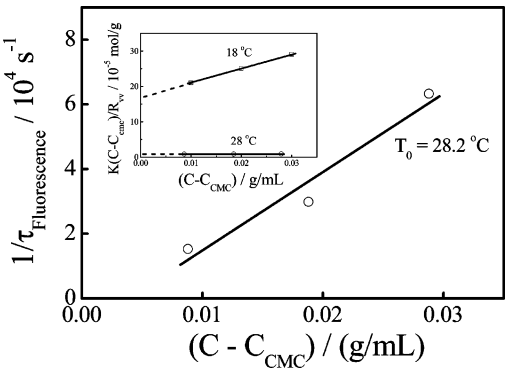

Figure 11. Copolymer concentration dependence of the characteristic transition time (τ) determined from the temperature jump-induced fluorescence intensity change, where $C_{CMC} = 1.2 \times 10^{-3}$ g/mL. The inset shows plots of $K(C-C_{CMC})/R_{vv}$ vs $(C-C_{CMC})$ for PE10300 in water at two different temperatures.

there is a distinct advantage to using a hydrophilic ANS probe in the current study of triblock PEO−PPO−PEO copolymers; namely, the change in ANS fluorescence intensity can reflect the incorporation of individual unimer chains into a micelle. The shorter τ shows that the fluorescence measurement has a higher sensitivity.

Figure 11 shows the concentration dependence of τ from the fluorescence measurements at 28 °C, where the τ values were interpolation by curve fitting. On the basis of the Aniansson−Wall formalism,[31,59,60] $(1/\tau_{fluorescence})$ is a linear function of the copolymer concentration (C)

$$\frac{1}{\tau_{\text{fluorescence}}} = \frac{k^-}{\delta^2} + \frac{k^+}{\langle N \rangle}(C - C_{\text{CMC}}) \qquad (3)$$

where k^+ and k^- are the association and dissociation rate constants, respectively, $\langle N \rangle$ and δ are the average aggregation number per micelle and the relative width of the aggregation number distribution, respectively. From the intercept of each line at $C = 0$ in the inset of Figure 11, we can respectively determine the values of M_w of individual chains and the resultant micelles at 28 °C to be 6.0×10^3 and 1.4×10^5 g/mol. Therefore, from LLS and DSC measurements, we know that $\langle N \rangle \approx 24$ at 28 °C and $C_{CMC} \approx 1.2 \times 10^{-3}$ g/mL. On the basis of eq 3, the slope of the line in Figure 11 leads to $k^+ \approx (6.8 \pm 1.0) \times 10^6$ mol^{-1} dm^3 s^{-1}, which is similar to values from the studies of other pluronics,[61] such as for P84 ($M_{PPO} = 2500$ g/mol and $W_{PEO} = 40\%$, EO_{19}-$PO_{43}EO_{19}$) at 27 °C with $k^+ \approx 1.8 \times 10^7$ mol^{-1} dm^3 s^{-1} and for L64 ($M_{PPO} = 1740$ g/mol and $W_{PEO} = 40\%$, $EO_{13}PO_{30}EO_{13}$) at 43 °C with $k^+ \approx 2.5 \times 10^8$ mol^{-1} dm^3 s^{-1}. The higher k^+ value can be attributed to a shorter PEO block or a shorter PPO block because a thin PEO corona makes the insertion of free copolymer chains into a micelle easier. The dissociation rate constant (k^-) deduced from C_{CMC} and k^+ by $C_{CMC} = k^-/k^+$ is $\sim 1.6 \times 10^3$ s^{-1}, smaller than 1.4×10^5 s^{-1} for L64.[37]

Conclusions

The thermodynamics as well as the micellization kinetics of purified poly(ethylene oxide)-*b*-poly(propylene oxide)-*b*-poly(ethylene oxide) triblock copolymer (Pluronic PE10300) can be effectively studied by a combination of ultrasensitive differential scanning calorimetry (US-DSC), laser light scattering (LLS),

(59) Aniansson, E. A. G.; Wall, S. N. *J. Phys. Chem.* **1974**, *78*, 1024.
(60) Aniansson, E. A. G.; Wall, S. N.; Almgren, M.; Hoffmann, H.; Kielmann, I.; Ulbricht, W.; Zana, R.; Lang, J.; Tondre, C. *J. Phys. Chem.* **1976**, *80*, 905.
(61) Zana, R.; Marques, C.; Johner, A. *Adv. Colloid Interface Sci.* **2006**, *123*, 345.

and fluorescence spectrometry with a hydrophilic fluorescent probe, 8-anilino-1-naphthalenesulfonic acid ammonium salt (ANS), and an ultrafast pulsed infrared heating laser. The critical micellization temperatures obtained in DSC, LLS, and fluorescence are similar. The heating pulse can induce micellization and lead to the incorporation of free copolymer chains into a micelle so that both the fluorescence and Rayleigh scattering intensities increase within a few milliseconds. Each intensity increase is well fitted by a single-exponential function and results in a characteristic transition time (τ). For a given initial temperature, τ decreases as the copolymer concentration increases (i.e., the incorporation becomes fast). However, τ decreases as the initial solution temperature increases for a given copolymer concentration. Even though $\tau_{\text{fluorescence}}$ and τ_{Rayleigh} take similar values as well as similar initial solution temperatures and copolymer concentration dependences, the fluorescence measurement with ANS as a probe is more sensitive and has a better signal-to-noise ratio than does Rayleigh scattering.

Acknowledgment. The financial support of the Chinese Academy of Sciences (CAS) Special Grant (KJCX2-SW-H14), the National Natural Scientific Foundation of China (NNSFC) Projects (20534020 and 20574065), and the Hong Kong Special Administration Region (HKSAR) Earmarked Project (CUHK4025/04P, 2160242) is gratefully acknowledged. We thank Professors Martin Gruebele and Shuqin Yu for their help in setting up the instrument and Mr. Yanwei Ding for DSC measurements.

Note Added after ASAP Publication. This article was released ASAP on August 18, 2007. Changes were made to the text, and the correct version was posted on August 22, 2007.

LA701626K